

Classical solutions and pattern formation for a volume filling chemotaxis model

Zhian Wang and Thomas Hillen

*Department of Mathematical and Statistical Science, University of Alberta,
Edmonton Alberta T6G 2G1, Canada*

(Received 2 February 2007; accepted 5 July 2007; published online 28 September 2007)

We establish the global existence of classical solutions to a generalized chemotaxis model, which includes the volume filling effect expressed through a nonlinear squeezing probability. This novel choice of squeezing probability reflects the elastic properties of cells. Necessary and sufficient conditions for spatial pattern formation are given and the underlying bifurcations are analyzed. In numerical simulations, the complex dynamics of merging and emerging patterns are shown for zero cell kinetics and nonzero cell kinetics, respectively. We conclude that the emerging process of pattern formation is due to cell growth. © 2007 American Institute of Physics.
[DOI: 10.1063/1.2766864]

Chemotaxis describes the active oriented movement of cells or other species along chemical gradients. The mathematical analysis of chemotaxis equations revealed a plentitude of spatial patterns, including aggregations, finite-time blowup, spot patterns, spikes, plateaus, or traveling waves. In this paper, we focus on the spatial patterns generated by the volume filling chemotaxis model. The volume filling model takes the finite volume of cells into account. We prove, for a very general class of volume filling models, that solutions exist globally in time and stay bounded; hence, no blowup is possible. By a novel choice of the so-called squeezing probability $q(u)$ we try to incorporate the semielastic properties of cells. Cells are not solid blocks, but they are deformable and elastic and can squeeze into openings. For this choice of squeezing probability q , we investigate the stability of the spatially homogeneous equilibrium, analyze the underlying bifurcations, and show numerical simulations. It turns out that the numerical solution without cell kinetics (no cell death or cell proliferation) shows a coarsening dynamics of merging of local peaks. This coarsening is well known from other phase-transition problems, for example, the Cahn-Hilliard equations. If cell kinetics are included, we observe complex dynamics of merging and emerging of local peaks. In many cases the dynamics does not appear to be periodic and we suspect that chaotic dynamics is possible. This, however, cannot be proven with the methods currently available.

I. INTRODUCTION

Chemotaxis is the characteristic movement or orientation of an organism or cell along a chemical concentration gradient either toward or away from the chemical stimulus. In the first case, the chemical is called a chemoattractant, and in the second case it is said to be a chemorepellent. The term chemotaxis is used broadly in the mathematical literature to describe general chemosensitive movement responses. Models for chemotaxis have been successfully applied to the aggregation patterns in bacteria,¹⁻³ slime molds,⁴ skin pigmen-

tation patterns,⁵ angiogenesis in tumor progression and wound healing,⁶ and many other examples. A classical and very important chemotaxis model was proposed by Keller and Segel⁷ in 1970 to describe the aggregation process of cellular slime mold by chemical attraction. A special case of the Keller-Segel model reads

$$\begin{aligned} u_t &= \nabla(\nabla u - u\chi(v) \nabla v), \quad (x,t) \in \Omega \times (0, \infty), \\ v_t &= \varepsilon \Delta v + g(u,v), \quad \frac{\partial u}{\partial n} = \frac{\partial v}{\partial n} = 0, \\ u(x,0) &= u_0(x), \quad v(x,0) = v_0(x), \end{aligned} \quad (1.1)$$

where Ω is a bounded domain of \mathbb{R}^n , $u(t,x)$ denotes the particle density, $v(t,x)$ stands for the concentration of chemoattractant, ε is a positive constant, χ is called chemosensitivity, and $g(u,v)$ describes production and degradation of the chemoattractant.

Model (1.1) has been extensively studied in great detail in the literature (e.g., see the survey articles of Hortsman^{8,9}). Of particular interest is the tendency of solutions to exhibit finite-time blowup. It has been shown that the possibility of blowup of the solutions to system (1.1) essentially depends on the space dimension. For constant chemosensitivity $\chi(v)=\chi$ and linear reproduction and degradation $g(u,v)=\nu u - \delta v$, finite-time blowup never happens in one dimension (unless there is no diffusion of the chemoattractant v) but can occur in n dimension for $n \geq 2$. The two-dimensional case is important and several thresholds (for radially symmetric solutions and for nonsymmetric solutions) were found. If the initial distribution exceeds this threshold, the solution will blow up in finite time. When the initial mass is below this threshold the solution exists globally.

There are various modifications of Eq. (1.1) which prevent blowup. For example, Mimura and Tsujikawa¹⁰ presented a chemotaxis-growth model, which reads

$$u_t = a\Delta u - \nabla(u\chi(v) \nabla v) + f(u) \quad \text{in } \Omega \times [0, \infty),$$

$$v_t = b\Delta v + vu - \delta v, \quad \frac{\partial u}{\partial n} = \frac{\partial v}{\partial n} = 0, \quad (1.2)$$

$$u(x, 0) = u_0(x), \quad v(0, x) = v_0(x),$$

where $f(u)$ is a smooth function of u such that $f(0)=0$ and

$$f(u) = (-\xi u + \zeta)u \quad \text{for sufficiently large } u.$$

The function $f(u)$ describes cell proliferation and cell death. For space dimension $n=1, 2$, Osaki *et al.*¹¹ showed that the solutions of problem (1.2) exist globally due to the dissipativity of the growth of cells. Moreover, saturation effects in the chemotactic component $\chi(v)$ occur very naturally if cell surface receptor kinetics is taken into account. Chemotaxis models with saturation effects can prevent blowup and have been used in many applications (Biler,¹² Ford *et al.*,¹³ Othmer and Stevens¹⁴). A chemotaxis model with finite sampling radius by incorporating a nonlocal sampling into the classical model was studied recently by Hillen *et al.*¹⁵ The global existence of the solution for any space dimension and numerical simulation of pattern formation is shown in Ref. 15. When cells demonstrate both chemoattraction and chemorepulsion according to multiple environmental signals, the classical model can be extended into an attraction-repulsion chemotaxis model. This type of model has been studied by a number of authors.¹⁶⁻¹⁸ The general conditions for blowup or global existence to some special cases of the attraction-repulsion model were identified in a recent work.¹⁹ Other strategies of preventing blowup are reviewed in a forthcoming paper.²⁰

Painter and Hillen¹⁷ introduced the mechanistic description of the volume filling effect. In the volume filling effect, it is assumed that particles have a finite volume and that cells cannot move into regions that are already filled by other cells. First, we give a brief derivation of the model below. For a full derivation we refer to Ref. 17.

The derivation of the model begins with a master equation for a continuous-time and discrete-space random walk (Othmer and Stevens¹⁴),

$$\frac{\partial u_i}{\partial t} = \mathcal{T}_{i-1}^+ u_{i-1} + \mathcal{T}_{i+1}^- u_{i+1} - (\mathcal{T}_i^+ + \mathcal{T}_i^-) u_i, \quad (1.3)$$

where \mathcal{T}_i^\pm are the transitional probabilities per unit of time for a one-step jump to $i \pm 1$.

In the volume filling approach, the probability of making a jump is assumed to depend on the availability of space into which cells can move. The transitional probability then takes the form

$$\mathcal{T}_i^\pm = q(u_{i\pm 1})(\alpha + \beta[\tau(v_{i\pm 1}) - \tau(v_i)]), \quad (1.4)$$

where $q(u)$ denotes the *squeezing probability* of a cell finding space at its neighboring location, α and β are constants, and τ represents the mechanism of the signal detection. It was assumed that only a finite number of cells, say \bar{u} , can be accommodated at any site, and the function q is stipulated by the condition

$$q(\bar{u}) = 0, \quad \text{with } 0 < q(u) \leq 1 \quad \text{for } 0 \leq u < \bar{u}.$$

Moreover, the squeezing probability is zero when the cell density exceeds \bar{u} . A logical immediate choice for $q(u)$ is

$$q(u) = \begin{cases} 1 - \frac{u}{\bar{u}}, & 0 \leq u \leq \bar{u}, \\ 0, & u > \bar{u}, \end{cases} \quad (1.5)$$

which says that the probability of a cell finding space at its neighboring site decreases linearly in the cell density at that site. The choice (1.5) for $q(u)$ corresponds to the interpretation that cells are solid blocks and the probability of finding space is proportional to the number of occupants (see Refs. 17, 21, and 22). However, cells are not solid blocks; they are elastic and can squeeze into openings. Hence the probability $q(u)$ of a cell finding space should be a nonlinear function, which is greater than a linear distribution. Under this consideration, a more realistic form of squeezing probability $q(u)$, which takes into account the elastic properties of cells, is

$$q(u) = \begin{cases} 1 - \left(\frac{u}{\bar{u}}\right)^\gamma, & 0 \leq u \leq \bar{u}, \\ 0, & u > \bar{u}, \end{cases} \quad (1.6)$$

where $\gamma \geq 1$ is called the *squeezing exponent* in this paper.

Substituting Eq. (1.4) into the master equation (1.3), applying Taylor expansion, and converting the discrete equation into a continuous equation, we end up with the following equation:

$$u_t = \nabla \cdot (d_1(q(u) - q'(u)u) \nabla u - q(u)u\chi(v) \nabla v), \quad (1.7)$$

where

$$d_1 = k\alpha, \quad \chi(v) = 2k\beta \frac{d\tau(v)}{dv},$$

and k is a scaling constant.

Another possible choice of squeezing probability $q(u)$, which also reflects elastic cell property, is given as

$$q(u) = \begin{cases} \left(1 - \frac{u}{\bar{u}}\right)^r, & 0 \leq u \leq \bar{u}, \\ 0, & u > \bar{u}, \end{cases} \quad (1.8)$$

with $0 < r < 1$. For this choice of $q(u)$, the derivative $q'(u) \rightarrow \infty$ as $u \rightarrow \bar{u}$, which leads to a singularity in the diffusion coefficient [see Eq. (1.7)]. In that case the model becomes a *fast diffusion* parabolic equation and the classical theory for global existence of nonlinear parabolic equations no longer applies. Hence we will use Eq. (1.6) as an example in the following analysis. We can, however, do a similar pattern formation analysis for Eq. (1.8) and also find merging and emerging dynamics similar, as Eq. (1.6) does (not shown here, but in Ref. 23).

If we combine the chemotaxis equation (1.7) with the dynamic equation for the external signal, and incorporate the birth and death dynamics of cells and external signals, denoted by $f(u, v)$ and $g(u, v)$, respectively, we obtain a formulation of the volume filling chemotaxis model,

$$u_t = \nabla \cdot (d_1(q(u) - q'(u)u) \nabla u - q(u)u\chi(v) \nabla v) + f(u,v), \tag{1.9}$$

$$v_t = d_2 \Delta v + g(u,v),$$

on a bounded smooth domain Ω . Moreover, the zero-flux boundary conditions are prescribed as follows:

$$(d_1(q(u) - q'(u)u) \nabla u) \cdot \mathbf{n} - q(u)u\chi(v) \nabla v \cdot \mathbf{n} = 0, \tag{1.10}$$

$$\nabla v \cdot \mathbf{n} = 0,$$

where \mathbf{n} denotes the unit outward normal vector at the boundary $\partial\Omega$.

The global existence of solutions to a volume filling chemotaxis model was first obtained in Ref. 24, where cell proliferation was not taken into account. Recently, Wrzosek²⁵ proved the global existence of the solution to system (1.9) and (1.10) with cell kinetics and a smooth squeezing probability $q(u)$. Furthermore, he proved the existence of a global attractor of system (1.9) and (1.10) in any space dimension $n \geq 1$ for the special linear form of $q(u)$ as in Eq. (1.5).³⁵ In this paper, we consider a more realistic squeezing probability $q(u)$, which reflects the semielastic property of cells and more general kinetic forms f and g . We prove the global existence of classical solutions and study pattern formation to system (1.9) and (1.10) under our novel choice of squeezing probability. For pattern formation, we extend the analysis in Ref. 17 by generalizing the squeezing probability function $q(u)$ to the form of Eq. (1.6) for $\gamma \geq 1$. It is worthwhile to note that the choice of Eq. (1.6) with $\gamma > 1$ in Eq. (1.9) results in density-dependent diffusion (nonlinear diffusion) in the first equation of Eq. (1.9), which is in contrast to choice Eq. (1.5) that results in a constant diffusion (linear diffusion).

The rest of the paper is organized as follows. In Sec. II, we give the basic assumptions for squeezing probability $q(u)$, as well as the kinetic functions f and g , and prove the global existence of classical solutions to the system (1.9) and (1.10). The results are obtained based on Amann's theory of parabolic systems²⁶⁻²⁸ by making a smooth extension for $q(u)$. In Sec. III, we will identify the conditions for pattern formation of the general system (1.9) with zero-flux boundary conditions (1.10) by performing the standard linear stability analysis. In Sec. IV, we consider Eq. (1.6) and derive the dispersion relation. Based on this dispersion relation, we investigate the bifurcations of the chemosensitivity χ , the growth rate ν , and the death rate δ of the chemoattractant. We also study the influence of crowding capacity γ on pattern formation. In Sec. V, we show numerical simulations for system (1.9) and (1.10) and compare the patterns obtained for the choice of Eq. (1.6) versus Eq. (1.5). We close with a discussion in Sec. VI.

II. GLOBAL EXISTENCE

To study the local and global existence of the solutions to problem (1.9) and (1.10), we assume that non-negative initial data are given,

$$u(x,0) = u_0(x) \geq 0, \quad v(x,0) = v_0(x) \geq 0, \quad \text{for } x \in \Omega. \tag{2.1}$$

Moreover, we make the following assumptions:

- (A1) d_1 and d_2 are positive constants, $\chi \in C^2(\mathbb{R}, \mathbb{R})$ and $\chi(v) > 0$;
- (A2) The squeezing probability $q(u) \in C^3([0, \bar{u}])$ satisfies the following conditions:
 - (1) There exists a critical number \bar{u} such that $q(0)=1$, $q(\bar{u})=0$, and $0 < q(u) < 1$ for $u \in (0, \bar{u})$, and $q(u)=0$ for all $u > \bar{u}$;
 - (2) $q(u)$ is nonincreasing, i.e., $q'(u) \leq 0$. Moreover, $|q'(u)|$ is bounded and $q''(u) \leq 0$ for all $u \in [0, \bar{u}]$.

Hereafter we call \bar{u} the *crowding capacity*.

- (A3) $f \in C^2(\mathbb{R} \times \mathbb{R})$ satisfies the quasipositivity condition, i.e., $f(0, v) \geq 0$ for $v \geq 0$. Moreover, there exists a constant $u_c > 0$ with $u_c < \bar{u}$ such that for all $v \geq 0$,

$$f(u_c, v) = 0 \quad \text{and} \quad f(u, v) < 0 \quad \text{for } u > u_c. \tag{2.2}$$

We call u_c the carrying capacity.

- (A4) $g \in C^2(\mathbb{R} \times \mathbb{R})$ is bounded and satisfies the quasipositivity condition $g(u, 0) \geq 0$ for $u \geq 0$. In addition, there exists a constant $\bar{v} > 0$ such that

$$g(u, \bar{v}) < 0 \quad \text{for } 0 \leq u \leq \bar{u}. \tag{2.3}$$

Standard examples for q are Eqs. (1.5) and (1.6). A typical choice for the cell kinetic function $f(u, v)$ is logistic growth $f(u, v) = \mu u(1 - u/u_c)$ and for g it is linear growth and death $g(u, v) = \nu u - \delta v$. A more general choice will be discussed later [see Eqs. (2.4) and (2.5)].

Remark 2.1. Here we assume that the crowding capacity \bar{u} is larger than the carrying capacity u_c . The carrying capacity denotes a critical density beyond which there is not enough nutrients available to support further population growth, whereas the crowding capacity gives only a volume constraint of how many particles can be squeezed into a unit area (or volume). Hence, it is reasonable to assume $\bar{u} > u_c$.

Remark 2.2. From Assumption (A2), we see that the squeezing probability function $q(u)$ is not differentiable at $u = \bar{u}$. Later on, we will show that the solution u satisfies $0 \leq u \leq \bar{u}$. So here $q'(\bar{u})$ represents the left derivative of $q(u)$ at $u = \bar{u}$, i.e., $q'(\bar{u}) = \lim_{u \rightarrow \bar{u}^-} q'(u)$.

Remark 2.3. The condition $q''(u) < 0$ for $0 \leq u \leq \bar{u}$ means $q(u)$ is concave in $[0, \bar{u}]$. So $q(u)$ is pointwise larger than the linear case in Eq. (1.5) for $u \in [0, \bar{u}]$, which is used to reflect the elastic properties of cells. As the same reasons stated in Remark 2.2, here we define $q''(\bar{u})$ as the left derivative of $q'(u)$ at $u = \bar{u}$. Note that the condition $q''(u) < 0$ is sufficient but not necessary for global existence.

Remark 2.4. We now compare the above assumptions (A1)–(A4) with the conditions imposed by Wrzosek in Refs. 25 and 35. In Ref. 25, $q(u) = \bar{q}(u)(\bar{u} - u)$ and $\bar{q}(u) > 0, \bar{q}(u) \in C^3(\mathbb{R})$ for all $u \in \mathbb{R}$. Clearly our assumptions are different from the assumptions in Ref. 25. The argument applied in Ref. 25 cannot be used directly here. Particularly, $q(u)$ is allowed to be not differentiable at $u = \bar{u}$ in our assumption. Even in the domain $[0, \bar{u}]$ in which $q(u)$ is smooth, our assumptions do not fulfill the assumptions in Ref. 25. For example, the choice of Eq. (1.6) for γ being an integer greater than 1 satisfies both our assumptions and Wrzosek's assumptions for $u \in [0, \bar{u})$. However, when $\gamma > 1$ is not an integer,

Eq. (1.6) cannot be represented in the form in Ref. 25 even for $u \in [0, \bar{u}]$.

For the cell kinetic term $f(u, v)$, in Ref. 25, $f(u, v) = uh(u)$ is independent of the chemoattractant concentration v , where $h(u) \leq 0$ for $u \geq \bar{u}$. However, the cell kinetics might depend on the concentration of the signal. Many growth factors have been shown to stimulate such dual activity; for example, vascular endothelial growth factor (VEGF) mediates both endothelial cell proliferation and chemotaxis. An example from Ref. 17 for this behavior is

$$f(u, v) = ruv \left(1 - \frac{u}{u_c} \right), \tag{2.4}$$

where it is assumed that the chemical mediates both cell migration and cell proliferation, where $u_c < \bar{u}$. For the signal kinetics $g(u, v)$, in Ref. 25, $g(u, v) = g_1(u) - v g_2(v)$, where $g_1, g_2 \in C^2(\mathbb{R}), g_1 \geq 0, g_1(0) = 0, g_2 \geq 0$ and $\lim_{y \rightarrow +\infty} y g_2(y) = +\infty$. In fact, $g(u, v)$ can be more general and the conditions can be relaxed to Eq. (2.3). A standard example is of birth-death structure, i.e.,

$$g(u, v) = g_1(u, v)u - g_2(u, v)v, \tag{2.5}$$

with bounded birth rate $g_1 \geq 0$ and death rate $g_2 \geq \kappa$ for some positive constant κ . Then, there exists a \bar{v} such that $g(u, v)$ satisfies condition (2.3).

Under the assumptions (A1)–(A4), we can immediately prove that v is non-negative and bounded above by \bar{v} , if $0 \leq u \leq \bar{u}$. This is shown in the following Lemma:

Lemma 2.5. *Let Assumptions (A1)–(A4) hold and (u, v) be a solution of system (1.9) and (1.10). If $0 \leq u \leq \bar{u}$, then it follows that $0 \leq v \leq \bar{v}$.*

Proof. We define an operator \mathbb{F} by

$$\mathbb{F}v = v_t - d_2 \Delta v - g(u, v).$$

Then $\underline{v} = 0$ is a lower solution of the v equation in Eq. (1.9) since for $0 \leq u \leq \bar{u}$,

$$\mathbb{F}\underline{v} = -g_1(u, 0) \leq 0,$$

and \bar{v} is a upper solution of the v equation due to

$$\mathbb{F}\bar{v} = -g(u, \bar{v}) > 0.$$

Then it follows from the comparison principle that $0 \leq v \leq \bar{v}$. \square

In what follows, we are devoted to proving the global existence of classical solutions to system (1.9) and (1.10). Note that $q(u)$ is not smooth at $u = \bar{u}$, which causes some trouble in applying the theory for nonlinear parabolic equations. Hence we first consider a smooth extension of $q(u)$, denoted by $\bar{q}(u)$, such that $\bar{q}(u) \in C^3(\mathbb{R})$ is concave and smooth at $u = \bar{u}$, and furthermore,

$$\bar{q}(u) = \begin{cases} 1, & u < 0, \\ q(u), & 0 \leq u \leq \bar{u}, \\ < 0, & u > \bar{u}. \end{cases}$$

Then we consider the following auxiliary problem:

$$u_t = \nabla \cdot (d_1(\bar{q}(u) - \bar{q}'(u)u) \nabla u - u\bar{q}(u)\chi(v) \nabla v) + f(u, v), \tag{2.6}$$

$$v_t = d_2 \Delta v + g(u, v).$$

Next, we will employ Amann’s results^{26–28} to prove the global existence of solutions to the auxiliary problem (2.6) and (1.10) and show that $0 \leq u \leq \bar{u}$ if $0 \leq u_0 \leq \bar{u}$. Since $q(u) = \bar{q}(u)$ for all $0 \leq u \leq \bar{u}$, and $0 \leq u \leq \bar{u}$ for $0 \leq u_0 \leq \bar{u}$, we automatically obtain the global existence of solutions for the original problem (1.9) and (1.10). The zero-flux boundary condition (1.10) is equivalent to the Neumann boundary condition. Amann’s results on global existence apply for both Dirichlet and Neumann boundary conditions. Hence, for a given function $\eta \in C(\partial\Omega, \{0, 1\})$, we consider more general conditions given by

$$\eta u + (1 - \eta) \frac{\partial u}{\partial \mathbf{n}} = 0 \quad \text{on } \partial\Omega, \tag{2.7}$$

$$\eta v + (1 - \eta) \frac{\partial v}{\partial \mathbf{n}} = 0 \quad \text{on } \partial\Omega,$$

where \mathbf{n} represents the outer unit normal vector on $\partial\Omega$.

Let $\rho \in (n, +\infty)$; then the space $W^{1,\rho}(\Omega; \mathbb{R}^2)$ is continuously embedded in the continuous function space $C(\Omega; \mathbb{R}^2)$. We define

$$W_b^{1,\rho} := \{w \in W^{1,\rho}(\Omega; \mathbb{R}^2) \mid \eta w|_{\partial\Omega} = 0\}.$$

By Assumption (A2) and the definition of the extension $\bar{q}(u)$, we know that $d(u) = d_1(\bar{q}(u) - \bar{q}'(u)u) > 0$ and $d(u)$ is smooth for $u \in \mathbb{R}$. Note that $\bar{q}(0) = 1$. Then it is easy to verify that there exists a $M > 0$ such that

$$d(u) > d_1 \quad \text{for } u \in [-M, M + \bar{u}]. \tag{2.8}$$

Now we can choose an open subset $\mathcal{G} \subset \mathbb{R}^2$ such that

$$X_1 \subset \mathcal{G} \subset X_2,$$

where

$$X_1 = \{(u, v) \in \mathbb{R}^2 \mid 0 \leq u \leq \bar{u}, \quad v \geq 0\}$$

and

$$X_2 = \{(u, v) \in \mathbb{R}^2 \mid -M \leq u \leq M + \bar{u}\}.$$

We consider the solution in the following solution space:

$$X := \{w = (u, v) \in W_b^{1,\rho} \mid w(\bar{\Omega}) \in \mathcal{G}\}.$$

Under the above mathematical setup, we have the following local existence theorem:

Lemma 2.6. *Let Ω be a smooth bounded domain of \mathbb{R}^n with boundary $\partial\Omega$ and the assumptions (A1)–(A4) be satisfied. Then we have*

(i) *For any initial data $(u_0, v_0) \in X$, there exists a positive constant $T(u_0, v_0)$ depending on the initial data (u_0, v_0) such that problem (2.6), (2.1), and (2.7) has a unique maximal classical solution $(u(x, t), v(x, t))$ defined on $\Omega \times (0, T(u_0, v_0))$ satisfying*

$$(u, v) \in C((0, T(u_0, v_0)); X) \cap C^{2,1}(\bar{\Omega} \times (0, T(u_0, v_0)); \mathbb{R}^2);$$

(ii) Let $\phi(t, (u_0, v_0))$ be the unique solution obtained above. Then ϕ is a $C^{0,1}$ -map from the set $\{(t, (u, v)) \mid (u, v) \in X, 0 \leq t \leq T(u_0, v_0)\}$ to X ;

(iii) If $u_0 \geq 0, v_0 \geq 0$, then $u \geq 0, v \geq 0$;

(iv) If $\|(u, v)(\cdot, t)\|_{L^\infty(\bar{\Omega})}$ is bounded away from the boundary of \mathcal{G} for each time t with $0 < t \leq T(u_0, v_0)$, then $T(u_0, v_0) = +\infty$, i.e., (u, v) is a global solution in time. Furthermore $(u, v) \in C^\theta([0, +\infty); C^{2(1-\sigma)}(\bar{\Omega}))$ for any $0 \leq \theta \leq \sigma < 1$.

Proof. The proof of local existence is similar to the proof in Refs. 25 and 29. Let $w = (u, v) \in \mathbb{R}^2$. Then Eqs. (1.9), (2.1), and (2.7) can be rewritten as

$$w_t = \nabla \cdot (a(w) \nabla w) + \mathcal{F}(w) \quad \text{in } \Omega \times [0, +\infty),$$

$$Bw = 0 \quad \text{on } \partial\Omega \times [0, +\infty), \tag{2.9}$$

$$w(\cdot, 0) = (u_0, v_0) \quad \text{in } \Omega,$$

where

$$a(w) = \begin{pmatrix} d_1(\bar{q}(u) - \bar{q}'(u)u) & -u\chi(v)\bar{q}(u) \\ 0 & d_2 \end{pmatrix}$$

and

$$Bw = \eta w - (1 - \eta) \frac{\partial w}{\partial \nu}.$$

Since for $(u, v) \in \mathcal{G}$, $d(u) = d_1(\bar{q}(u) - \bar{q}'(u)u) > 0$, the eigenvalues of $A(w)$ are positive. Therefore Eq. (2.9) is normally elliptic.²⁶ Then (i) and (ii) follow from Theorem 7.3 and Corollary 9.3 in Ref. 26. The positivity (iii) follows from Theorem 15.1 of Ref. 28. Since Eq. (2.9) is a triangular system, (iv) follows from Theorem 5.2 of Ref. 27. \square

To obtain the global solution, from the results in (iv) of Lemma 2.6, it remains to prove that u, v are L^∞ bounded away from the boundary of \mathcal{G} . By the definition of \mathcal{G} , it suffices to show that u is bounded below by 0 and above by \bar{u} . In the following lemma, we show that $0 \leq u \leq \bar{u}$, provided that $0 \leq u_0 \leq \bar{u}$.

Lemma 2.7. Assume that $0 \leq u_0 \leq \bar{u}$. Let (u, v) be a solution obtained in Lemma 2.6 with zero-flux boundary condition Eq. (1.10). Then it follows that $0 \leq u \leq \bar{u}$.

Proof. We use a comparison principle for nonlinear parabolic equation to prove the existence of upper and lower bounds for u . Indeed, the lower bound 0 has been obtained in Lemma 2.6 (iii). We only need to show the existence of the upper bound \bar{u} . Given $v \in C^{2,1}(\bar{\Omega} \times (0, T(u_0, v_0)))$, we can easily verify from the first equation of system (2.6) that the operator P is uniformly parabolic (see Ref. 30) on $\Gamma = \mathbb{R} \times \mathbb{R}^n \times \mathbb{R} \times \mathbb{R}$, where

$$Pu = P(u, \nabla u, \Delta u, u)$$

$$= u_t - \nabla \cdot (d_1(\bar{q}(u) - \bar{q}'(u)u) \nabla u - u\bar{q}(u)\chi(v) \nabla v)$$

$$- f(u, v).$$

For any solution (u, v) of system (2.6) obtained in Lemma 2.6, we have $Pu = 0$. However, for $u = \bar{u}$, we have from Assumptions (A2) and (A3) that

$$P\bar{u} > 0.$$

On the boundary $\partial\Omega$, we have $\partial\bar{u}/\partial\mathbf{n} = 0$. Hence $u = \bar{u}$ is a supersolution of system (2.6) with Neumann boundary conditions. Following the comparison principle, we obtain that $u \leq \bar{u}$. Together with the positivity property obtained in Lemma 2.6, one has $0 \leq u \leq \bar{u}$. \square

Note that for $0 \leq u \leq \bar{u}$, we have $\bar{q}(u) = q(u)$. Then combining Lemmas 2.5, 2.6, and 2.7, we obtain the following global existence and boundedness theorem to system (1.9) with zero-flux boundary condition (1.10).

Theorem 2.8. For any $(u_0, v_0) \in X$ with $0 \leq u_0 \leq \bar{u}$, $0 \leq v_0 \leq \bar{v}$ on $\bar{\Omega}$, the initial-boundary value problem (1.9), (1.10), and (2.1) has a unique positive solution (u, v) satisfying

- (i) $(u, v) \in C([0, +\infty); X) \cap C^{2,1}(\bar{\Omega} \times (0, +\infty); \mathbb{R}^2)$;
- (ii) $u(t, x)$ and $v(t, x)$ are bounded on $\bar{\Omega} \times [0, +\infty)$ with $0 \leq u \leq \bar{u}$, $0 \leq v \leq \bar{v}$;
- (iii) The solution semigroup $\phi(t, (u_0, v_0))$ forms a semidynamical system on X .

III. PATTERN FORMATION

Pattern formation in mathematics refers to the process that, by changing a bifurcation parameter, the spatially homogeneous steady states lose stability to spatially inhomogeneous perturbations, and stable inhomogeneous solutions arise. In this section, we investigate pattern formation for system (1.9). The approach applied here is very routine. We look for the spatial homogeneous steady states by setting the kinetics on the right-hand side of Eq. (1.9) to be zero,

$$f(u_s, v_s) = 0, \quad g(u_s, v_s) = 0. \tag{3.1}$$

We suppose that (u_s, v_s) is a non-negative solution of Eq. (3.1). That is (u_s, v_s) is a homogeneous steady state of system (1.9). We assume that in the absence of any spatial variation the homogeneous steady state is linearly stable. We first determine the conditions for this to hold.

With no spatial variation, u and v satisfy

$$u_t = f(u, v), \quad v_t = g(u, v). \tag{3.2}$$

The linearization of Eq. (3.2) at (u_s, v_s) is

$$w_t = Aw, \quad A = \begin{pmatrix} f_u & f_v \\ g_u & g_v \end{pmatrix}, \tag{3.3}$$

where A is the community (Jacobian) matrix of system (3.2) at steady state (u_s, v_s) . Hereafter, we shall take the partial derivative of f and g to be evaluated at the steady state unless stated otherwise. Then the conditions for which (u_s, v_s) is linearly stable can be easily determined by

$$\text{tr } A = f_u + g_v < 0, \quad |A| = f_u g_v - f_v g_u > 0. \tag{3.4}$$

If there are some parameters in f and g , then the steady states (u_s, v_s) are functions of these parameters. Hence, inequalities (3.4) impose certain constraints on the parameters.

In what follows, we shall consider the full chemotaxis model (1.9). We examine small perturbations from the spatially homogeneous steady state (u_s, v_s) of the form

$$u = u_s + \epsilon \tilde{u}(x, t), \quad v = v_s + \epsilon \tilde{v}(x, t), \tag{3.5}$$

where $\epsilon \ll 1$.

Substituting Eq. (3.5) into Eq. (1.9), we end up with

$$\begin{aligned} \epsilon \tilde{u}_t &= \epsilon \nabla (d_1(q(u_s + \epsilon \tilde{u}) - q'(u_s + \epsilon \tilde{u})(u_s + \epsilon \tilde{u})) \nabla u \\ &\quad - \epsilon(u_s + \epsilon \tilde{u})\chi(v_s + \epsilon \tilde{v})q(u_s + \epsilon \tilde{u}) \nabla \tilde{v}) \\ &\quad + f(u_s + \epsilon \tilde{u}, v_s + \epsilon \tilde{v}), \tag{3.6} \\ \epsilon \tilde{v}_t &= \epsilon d_2 \Delta \tilde{v} + g(u_s + \epsilon \tilde{u}, v_s + \epsilon \tilde{v}). \end{aligned}$$

Equating first-order terms with respect to ϵ , neglecting higher-order terms, and dropping the tilde for the convenience, we obtain the following linearized system for Eq. (1.9):

$$\begin{aligned} u_t &= d_1(q(u_s) - q'(u_s)u_s) \Delta u - u_s q(u_s) \chi(v_s) \Delta v + u f_u + v f_v, \tag{3.7} \\ v_t &= d_2 \Delta v + u g_u + v g_v. \end{aligned}$$

Hereafter we abbreviate $\vartheta = q(u_s) - q'(u_s)u_s$ and $\varrho = -\chi(v_s)u_s q(u_s)$. The v_s in $\chi(v_s)$ will be often abbreviated for notational convenience unless stated otherwise, i.e., $\chi = \chi(v_s)$. Since we assume that $q'(u) < 0$ for $0 \leq u \leq \bar{u}$, we have $\vartheta > 0$. The chemotactic sensitivity χ is always assumed to be non-negative and hence $\varrho < 0$.

In the following, we assume that the domain is a one-dimensional bounded domain, similar analysis holds for higher dimensional bounded domains. Then following the standard argument (e.g., see Ref. 31), the dispersion relation associated with system (3.7) can be determined as

$$\lambda^2 + a(k^2)\lambda + b(k^2) = 0, \tag{3.8}$$

where k is the spatial eigenvalue, which is commonly referred to as the wave number, and λ is the eigenvalue, which determines temporal growth and depends on the wave number k . The $a(k^2)$ and $b(k^2)$ are given, respectively, as

$$\begin{aligned} a(k^2) &= (\vartheta d_1 + d_2)k^2 - (f_u + g_v), \tag{3.9} \\ b(k^2) &= \vartheta d_1 d_2 k^4 + (\varrho g_u - d_2 f_u - \vartheta d_1 g_v)k^2 + f_u g_v - f_v g_u. \end{aligned}$$

The dispersion relation (3.8) gives $\lambda(k)$ as a function of wave number k at steady state (u_s, v_s) . For the steady state to be unstable, we require that $Re\lambda(k)$ is positive for some $k \neq 0$. Since $a(k^2) > 0$ due to Eq. (3.4), the instability can only occur if $b(k^2)$ becomes negative for some k so that Eq. (3.8) for λ has one positive and one negative root. Referring to Eq. (3.9), the condition $b(k^2) < 0$ requires that

$$\vartheta d_1 d_2 k^4 + (\varrho g_u - d_2 f_u - \vartheta d_1 g_v)k^2 + f_u g_v - f_v g_u < 0. \tag{3.10}$$

Since it is required in Eq. (3.4) that $|A| = f_u g_v - f_v g_u > 0$, a necessary condition for Eq. (3.10) is

$$\varrho g_u - d_2 f_u - \vartheta d_1 g_v < 0. \tag{3.11}$$

For Eq. (3.10) to be the case for some nonzero k , the discriminant of equation $b(k^2) = 0$ must be positive since the coefficient $\vartheta d_1 d_2$ of k^4 is positive. In other words, for the existence of an interval of unstable modes, we require that

$$(\varrho g_u - d_2 f_u - \vartheta d_1 g_v)^2 - 4\vartheta d_1 d_2 (f_u g_v - f_v g_u) > 0. \tag{3.12}$$

Applying Eq. (3.11), we obtain from Eq. (3.12) that

$$\varrho g_u - d_2 f_u - \vartheta d_1 g_v < -2\sqrt{\vartheta d_1 d_2 (f_u g_v - f_v g_u)}. \tag{3.13}$$

To recap, we have now obtained conditions for the generation of spatial patterns for the volume filling chemotaxis model (1.9) and (1.10). For convenience, we reproduce them here. Remembering that all derivatives are evaluated at the steady state (u_s, v_s) , they are

$$\begin{aligned} f_u + g_v &< 0, \quad f_u g_v - f_v g_u > 0, \quad \varrho g_u - d_2 f_u - \vartheta d_1 g_v < 0, \tag{3.14} \\ (\varrho g_u - d_2 f_u - \vartheta d_1 g_v)^2 &- 4\vartheta d_1 d_2 (f_u g_v - f_v g_u) > 0, \end{aligned}$$

where $\vartheta = q(u_s) - q'(u_s)u_s$, $\varrho = -\chi(v_s)u_s q(u_s)$. The importance of the chemotaxis term in the chemotaxis model is that it leads to a Δv term in the u equation, so-called cross diffusion. This removes the need for d_1 and d_2 to be sufficiently different in order to obtain spatial patterns. The strength of the chemotactic sensitivity χ plays a crucial role in pattern formation. Generally there exists a critical value χ_c such that there is no pattern formation if χ is below this critical value χ_c , while pattern formation can be expected if χ is larger than this critical value χ_c . In our problem, we can explicitly determine this critical value if all parameters are fixed in system (1.9) except for the chemotactic sensitivity χ . Indeed, from the foregoing analysis, we know that the bifurcation occurs when

$$\varrho g_u - d_2 f_u - \vartheta d_1 g_v = -2\sqrt{\vartheta d_1 d_2 (f_u g_v - f_v g_u)}. \tag{3.15}$$

Substituting $\varrho = -\chi u_s q(u_s)$ into Eq. (3.15) and solving the resulting equation for χ , we obtain the critical chemosensitivity χ_c ,

$$\chi_c = \frac{2\sqrt{\vartheta d_1 d_2 (f_u g_v - f_v g_u)} - d_2 f_u - \vartheta d_1 g_v}{g_u u_s q(u_s)}. \tag{3.16}$$

At this bifurcation value, the corresponding critical wave-number is given by

$$k_c^2 = \frac{d_2 f_u + \vartheta d_1 g_v - \varrho g_u}{2\vartheta d_1 d_2}. \tag{3.17}$$

Whenever $b(k^2) < 0$, Eq. (3.8) has a solution λ , which is positive for the range of wave numbers. When $\chi > \chi_c$, from Eq. (3.9), the range of unstable wave numbers $k_1^2 < k^2 < k_2^2$ is obtained from the zeros k_1^2 and k_2^2 of $b(k^2) = 0$ as

$$\begin{aligned} k_1^2 &= \frac{C - \{C^2 - 4\vartheta d_1 d_2 (f_u g_v - f_v g_u)\}^{1/2}}{2\vartheta d_1 d_2} < k^2, \\ < k_2^2 &= \frac{C + \{C^2 - 4\vartheta d_1 d_2 (f_u g_v - f_v g_u)\}^{1/2}}{2\vartheta d_1 d_2}, \tag{3.18} \end{aligned}$$

where $C = d_2 f_u + \vartheta d_1 g_v - \varrho g_u$ denotes the coefficient of k^2 in the equation $b(k^2) = 0$ [Eq. (3.9)].

Whenever conditions (3.14) are satisfied and there is a range of wave numbers k lying within the bound defined by Eq. (3.18), then the corresponding spatial eigenfunctions are linearly unstable and pattern formation can be expected. It is worthwhile to point out that for an infinite domain there is

always a spatial pattern if $0 < k_1^2 < k_2^2$ in Eq. (3.18). In this situation, conditions (3.14) are sufficient conditions for pattern formation to system (1.9) and (1.10), while for a finite domain, the possible wave numbers k and corresponding spatial wavelengths are discrete and depend in part on the boundary conditions. If there does not exist a discrete wave number k^2 lying between k_1^2 and k_2^2 , then there is no spatial pattern formation even if Eq. (3.14) is satisfied. Some examples will be given in the forthcoming sections.

We summarize the main results obtained in this section in the following theorem.

Theorem 3.1. *Let (u_s, v_s) be a spatially homogeneous steady state of system (1.9). Let f_u, f_v and g_u, g_v denote the partial derivatives evaluated at steady state (u_s, v_s) . Then pattern formation of system (1.9) with zero-flux boundary condition (1.10) is possible if Eq. (3.14) is satisfied. Furthermore, the critical chemosensitivity χ_c is determined by Eq. (3.16). When $\chi < \chi_c$, there is no spatial pattern, whereas pattern formation can be expected if $\chi > \chi_c$ and the range of unstable wave numbers is given by Eq. (3.18).*

IV. ANALYSIS FOR NONLINEAR SQUEEZING PROBABILITY

By the global existence and boundedness obtained in Theorem 2.4, we know that $0 \leq u \leq \bar{u}$ if $0 \leq u_0 \leq \bar{u}$. Then, as we mentioned in the Introduction, a logical choice for the squeezing probability function $q(u)$, which reflects the elastic property of particles, is

$$q(u) = 1 - \left(\frac{u}{\bar{u}}\right)^\gamma, \quad \gamma \geq 1, \quad 0 \leq u \leq \bar{u}. \tag{4.1}$$

In this section, we will discuss the dynamics of system (1.9) with $q(u)$, which has the nonlinear form (4.1). For simplicity, we suppose that the cell and chemoattractant kinetics have the following form extensively used in literature (e.g., Refs. 17 and 25):

$$f(u, v) = \mu u(1 - u/u_c), \quad g(u, v) = \nu u - \delta v, \tag{4.2}$$

where the cell kinetics follows the logistic growth with carrying capacity $0 < u_c \leq \bar{u}$ and $\mu > 0$; the chemoattractant grows with rate ν and decays with rate δ due to dilution. Applying Eqs. (4.1), (4.2), and (1.9), we obtain

$$\begin{aligned} u_t &= \nabla \cdot (D(u) \nabla u - \chi \varphi(u) \nabla v) + \mu u \left(1 - \frac{u}{u_c}\right), \\ v_t &= d_2 \Delta v + \nu u - \delta v, \end{aligned} \tag{4.3}$$

$$(D(u) \nabla u - \chi \varphi(u) \nabla v) \cdot \mathbf{n} = 0, \quad \nabla v \cdot \mathbf{n} = 0,$$

where \mathbf{n} , as usual, denotes the unit outward normal vector at the boundary of the domain and $D(u)$ and $\varphi(u)$ are denoted by

$$D(u) = d_1 \left[1 + (\gamma - 1) \left(\frac{u}{\bar{u}}\right)^\gamma \right], \quad \varphi(u) = u \left[1 - \left(\frac{u}{\bar{u}}\right)^\gamma \right]. \tag{4.4}$$

As a special case of Eq. (1.9), the global existence and boundedness of the solution to Eq. (4.3) has been given by Theorem 2.4.

Clearly, the spatially homogeneous steady states of system (4.3) are $(0, 0)$ and $(u_c, \nu u_c / \delta)$. Furthermore, by linearization, one can easily determine that the steady state $(0, 0)$ is a saddle point and hence unstable, while the steady state $(u_c, \nu u_c / \delta)$ is stable to the corresponding homogeneous system of Eq. (4.3) with two negative eigenvalues $-\nu$ and $-\delta$. Therefore, we focus on the stable steady state $(u_s, v_s) = (u_c, \nu u_c / \delta)$ to study pattern formation for system (4.3). First, we linearize system (4.3) about the steady state $(u_c, \nu u_c / \delta)$ and obtain

$$u_t = \nabla \cdot (D(u_c) \nabla u) - \nabla \cdot (\chi \varphi(u_c) \nabla v) - \mu u,$$

$$v_t = d_2 \Delta v + \nu u - \delta v.$$

Performing the linear stability analysis as before, we find the corresponding dispersion relation

$$\begin{aligned} \lambda^2 + a(k^2)\lambda + b(k^2) &= 0, \\ a(k^2) &= (D(u_c) + d_2)k^2 + (\mu + \delta), \end{aligned} \tag{4.5}$$

$$b(k^2) = D(u_c)d_2k^4 + (\mu d_2 + \delta D(u_c) - \chi \nu \varphi(u_c))k^2 + \mu \delta.$$

From the analysis in the previous section, the condition (3.14) has to be satisfied to obtain pattern formation. In the situation discussed in this section, we know that $f_u + g_v = -(\mu + \delta) < 0$ and $f_u g_v - f_v g_u = \mu \delta > 0$. Then we only need the third and fourth condition in Eq. (3.14) to hold. This requires that [see Eq. (3.13)]

$$\mu d_2 + \delta D(u_c) - \chi \nu \varphi(u_c) < -2\sqrt{d_2 \mu \delta D(u_c)}. \tag{4.6}$$

Then Eq. (4.6) gives a necessary condition for pattern formation of system (4.3). If we regard the wave number as a continuous variable in spite of the fact that the wave number is discrete, Eq. (4.6) then gives a sufficient and necessary condition for pattern formation of system (4.3) with zero-flux boundary condition.

In the remainder of this section, we will investigate the influence of the squeezing exponent γ , chemosensitivity χ , growth rate ν , and death rate δ of chemoattractant on the pattern formation of Eq. (4.3).

A. Bifurcations with chemotactic sensitivity χ

From the previous analysis, if we think of the chemosensitivity χ as the bifurcation parameter, then the bifurcation value χ_c is determined by [see Eq. (3.16)]

$$\chi_c = \frac{2\sqrt{d_2 \mu \delta D(u_c)} + \mu d_2 + \delta D(u_c)}{\nu \varphi(u_c)}. \tag{4.7}$$

The corresponding critical wave number k_c is determined from Eq. (3.17) by

$$k_c^2 = \frac{-\mu d_2 - \delta D(u_c) + \chi_c \nu \varphi(u_c)}{2d_2 D(u_c)}. \tag{4.8}$$

When $\chi > \chi_c$, we have $b(k^2) < 0$ for some wave numbers k^2 and hence there exists a positive solution λ of Eq. (4.5) for some $k \neq 0$. Moreover, the range of unstable wave numbers $k_1^2 < k^2 < k_2^2$ can be obtained as

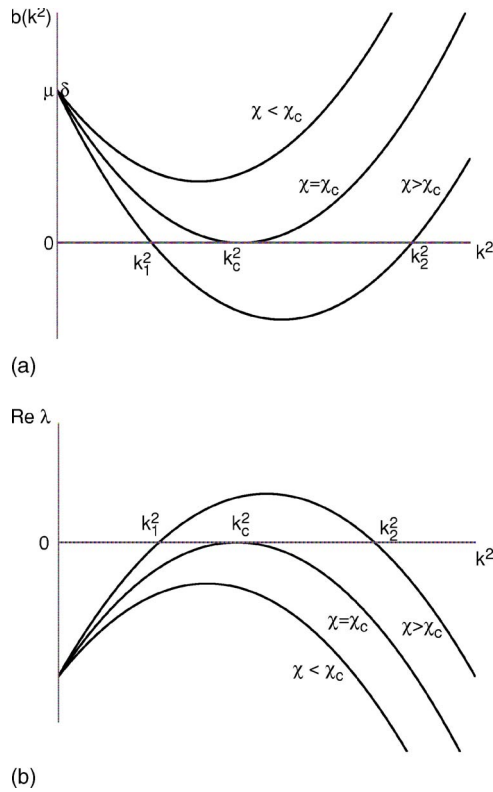


FIG. 1. (a) A sketch of $b(k^2)$ against k^2 defined by Eq. (4.5). When the chemosensitivity strength χ increases beyond the critical value χ_c , $b(k^2)$ becomes negative for a finite range of k^2 . (b) Plot of the real part of eigenvalue $\lambda(k^2)$ as a function of k^2 defined in Eq. (4.5). When $\chi > \chi_c$, there is a range of wave numbers $k_1^2 < k^2 < k_2^2$ such that the steady state is unstable. The parameters are chosen as $\gamma=1$, $d_1=0.1$, $d_2=1.0$, $u_c=2.0$, $\bar{u}=4.0$, $\mu=4.0$, $\nu=5.0$, $\delta=10.0$.

$$k_1^2 = \frac{S - \{S^2 - 4\mu\delta d_2 D(u_c)\}^{1/2}}{2d_2 D(u_c)} \tag{4.9}$$

and

$$k_2^2 = \frac{S + \{S^2 - 4\mu\delta d_2 D(u_c)\}^{1/2}}{2d_2 D(u_c)}, \tag{4.10}$$

where $S = -\mu d_2 - \delta D(u_c) + \chi \nu \varphi(u_c)$.

Then the critical value is (k_c, χ_c) such that $b(k^2) > 0$ for all k^2 if $\chi < \chi_c$, however, $b(k^2) < 0$ for a range of wave numbers $k_1^2 < k^2 < k_2^2$ if $\chi > \chi_c$. Figure 1(a) shows how $b(k^2)$ varies as a function of k^2 for various χ and Fig. 1(b) shows how the eigenvalue λ varies as a function of k^2 for various χ . A stability curve for $b(k^2)=0$ for $\gamma=2$ in Fig. 2 immediately gives us some information we need to know. When $\chi \leq \chi_c$, $b(k^2) \geq 0$, and consequently, no positive wave numbers correspond to χ . As χ increases and exceeds the critical value χ_c , there must exist wave numbers k between the two curves (dashed and solid portion of the curve in Fig. 2). These wave numbers define unstable modes.

As we mentioned in the previous section, the condition $\chi > \chi_c$ does not guarantee pattern formation since the allowable wave numbers k are discrete for a finite domain. Generally, the pattern formation can be achieved by increasing the domain size. So a question arises as to how a necessary and sufficient condition can be derived to generate the spatial

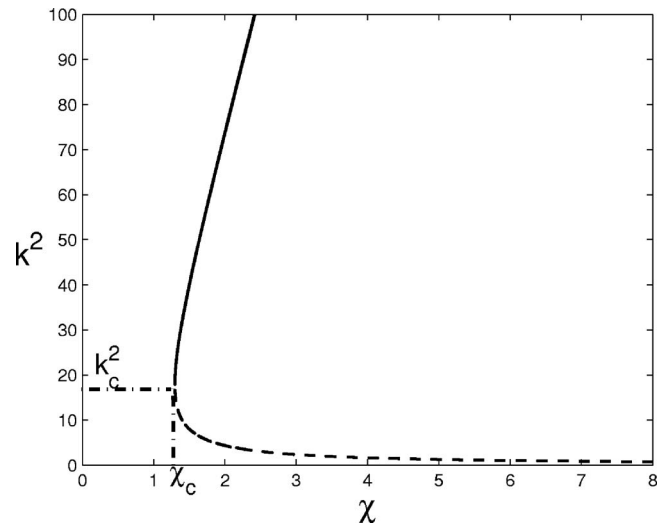


FIG. 2. A sketch of $b(k^2)=0$ in Eq. (4.5) in the (k^2, χ) plane, where parameters are chosen as $\gamma=2$, $d_1=0.1$, $d_2=1.0$, $u_c=2.0$, $\bar{u}=4.0$, $\mu=4.0$, $\nu=5.0$, $\delta=10.0$, and consequently, $k_c^2=17.889$, $\chi_c=1.296$. The dashed portion denotes k_1^2 and the solid portion represents k_2^2 .

pattern for a fixed domain. Indeed, the bifurcation diagram, Fig. 2, has given us some useful clues already. We study the difference for k_2^2 and k_1^2 ,

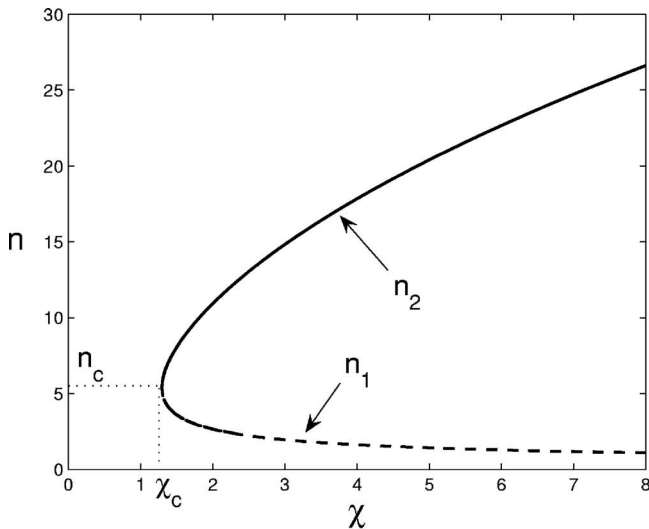
$$\begin{aligned} \mathcal{K}(\chi, \nu, \delta) &= k_2^2 - k_1^2 \\ &= \frac{[(\mu d_2 - \delta D(u_c) + \nu \chi \varphi(u_c))^2 - 4\mu\delta d_2 D(u_c)]^{1/2}}{d_2 D(u_c)}. \end{aligned}$$

Here we consider the difference as a function of χ , ν , and δ , since we will investigate the influence of χ , ν , and δ on the pattern formation in the following. It is easy to verify that $\mathcal{K}(\chi, \nu, \delta)$ is an increasing function of χ and ν . So pattern formation can be supported by increasing the value of χ or ν . Biologically, we expect pattern formation if the growth rate ν of the chemoattractant or the chemosensitivity χ is big enough. On the other hand, $\mathcal{K}(\chi, \nu, \delta)$ is a decreasing function of δ . Hence pattern formation also can be supported by decreasing the decay rate δ of the signal.

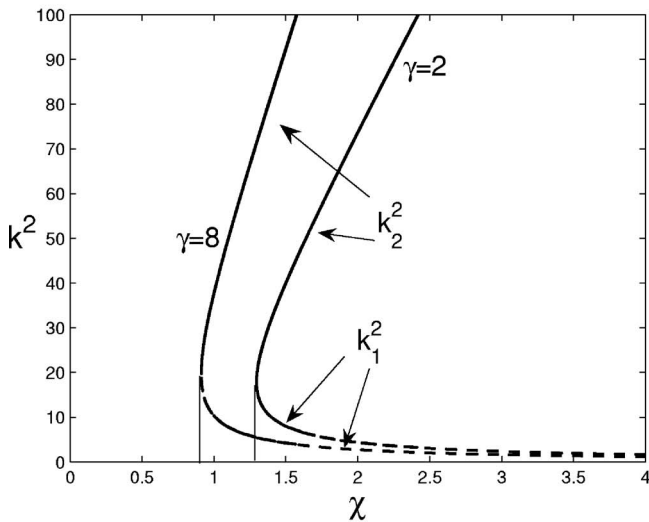
We now derive a sufficient and necessary condition for the chemosensitivity χ for pattern formation in a one-dimensional domain $[0, \ell]$. On $[0, \ell]$ with non-flux-boundary conditions, the corresponding wave numbers k are given by $k=n\pi/\ell$, where $n=0, \pm 1, \pm 2, \dots$. The requirement (3.18) in terms of modes n becomes

$$n_1^2 < n^2 < n_2^2, \tag{4.11}$$

where $n_1 = k_1 \ell / \pi$ and $n_2 = k_2 \ell / \pi$. Now we want to find an appropriate value of χ such that there exists at least one integer n satisfying Eq. (4.11). Without loss of generality, we look at positive wave modes only and other cases can be analyzed analogously. For $\chi = \chi_c$, we have $k_1 = k_2 = k_c$ and hence $k_1 \ell / \pi = k_2 \ell / \pi$. We can easily check that $k_1^2(\chi)$ as a function of χ is decreasing and that $k_2^2(\chi)$ is increasing. As a consequence, n_1 is decreasing [see dotted portion of the curve in Fig. 3(a)] and n_2 is increasing [see solid portion of the curve in Fig. 3(a)] as a function of χ . Now we look for the conditions such that there exists at least one integer n



(a)



(b)

FIG. 3. (a) A sketch of $b(n^2\pi^2/\ell^2)=0$ in Eq. (4.5) in the (n, χ) plane, where the domain is chosen as $[0, \ell]$ with $\ell=4$ and parameters are chosen as $\gamma=2, d_1=0.1, d_2=1.0, u_c=2.0, \bar{u}=4.0, \mu=4.0, \nu=5.0, \delta=10.0$, and consequently, $n_c=5.38, \chi_c=1.296$. (b) A comparison of wave numbers with respect to squeezing exponent γ . Parameters are chosen as in (a) except γ .

between n_1 and n_2 . At the critical value χ_c as obtained above, we define $n_c := n_1(\chi_c) = n_2(\chi_c)$. Then we have two cases to consider.

Case (a). n_c is an integer. Then we increase χ from χ_c , and any increment of χ will lead to $n_1(\chi) < n_c < n_2(\chi)$ due to the monotonicity of n_1 and n_2 . We immediately get an unstable mode $n = n_c$ [see Fig. 3(a)]. In this case, χ_c is a bifurcation value, such that pattern formation is obtained when $\chi > \chi_c$ and no pattern formation evolves when $\chi < \chi_c$.

Case (b). n_c is not an integer number. Since $n_1(\chi)$ is continuously decreasing with respect to χ and $n_2(\chi) \rightarrow \infty$ as $\chi \rightarrow \infty$, there must exist a minimum number of χ , denoted by χ_B , such that $\chi_B > \chi_c$ and $n_1(\chi_B)$, or $n_2(\chi_B)$, or both, are integers. For $\chi > \chi_B$, we obtain an unstable mode n such that $n_1(\chi) < n < n_2(\chi)$.

We therefore end up with the following theorem.

Theorem 4.1. Assume $\gamma \geq 1$. Let $\chi_B \geq \chi_c$ be the first

number of χ such that either $k_1 \ell / \pi$, or $k_2 \ell / \pi$ is an integer. Then χ_B is a bifurcation number and $\chi > \chi_B$ is a necessary and sufficient condition for pattern formation of system (4.3).

Next, we examine the relationship between the critical value χ_c and the squeezing exponent γ , from which we can understand the influence of γ on the dynamics of system (4.3). We give the following theorem.

Theorem 4.2. The critical value χ_c , as a function of squeezing exponent γ , is decreasing.

Proof. For convenience, we denote $\sigma = u_c/\bar{u} < 1$ and $M(\gamma) = 1/(1 - (u_c/\bar{u})^\gamma) = 1/(1 - \sigma^\gamma) > 1$, then Eq. (4.7) can be rewritten as

$$\chi_c = \frac{1}{\nu u_c} \left(2\sqrt{\mu\delta d_1 d_2 M(\gamma)} \sqrt{1 + \gamma\sigma^\gamma M(\gamma)} + \mu d_2 M(\gamma) + \delta d_1 (1 + \gamma\sigma^\gamma M(\gamma)) \right). \tag{4.12}$$

Note that $0 < u_c/\bar{u} < 1$. Then function M is nonincreasing with respect to γ . Next we prove that function $\gamma\sigma^\gamma M(\gamma)$ is a decreasing function of γ . To see this, we define $h(\gamma) = \gamma\sigma^\gamma M(\gamma)$. Then we have

$$\frac{dh}{d\gamma} = \frac{\sigma^\gamma(1 - \sigma^\gamma + \gamma \ln \sigma)}{(1 - \sigma^\gamma)^2}.$$

Since $\sigma < 1$, it is easy to verify that $1 - \sigma^\gamma + \gamma \ln \sigma < 0$ for all $\gamma > 1$. So $h(\gamma)$ is decreasing with respect to γ . Consequently, the critical chemosensitivity value χ_c is a decreasing function of squeezing exponent γ . \square

Remark 4.3. Biologically, Theorem 4.2 tells us that cells are apt to aggregate when the squeezing exponent γ is increased, since the squeezing probability $q(u)$ is increasing with respect to γ . When the squeezing probability is bigger, cells are more motile and hence pattern formation is easier to form.

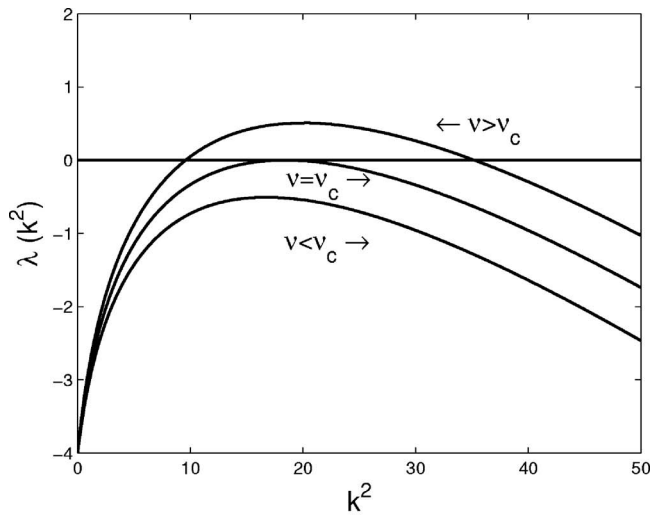
B. Bifurcation with growth rate ν

In this section, we consider growth rate ν as the bifurcation parameter, and therefore fix all other parameters in system (4.3). Note that varying ν affects the value of the steady state (u_s, v_s) . We want to understand the influence of the dynamical parameter ν on pattern formation of system (4.3). The temporal eigenvalues λ of the linearization at (u_s, v_s) are the roots of Eq. (4.5).

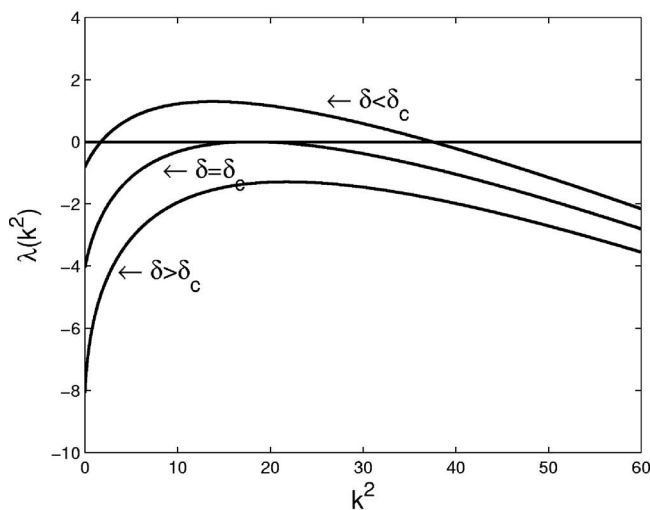
We compute the critical value ν_c for ν from Eq. (4.5),

$$\nu_c = \frac{2\sqrt{d_2\mu\delta D(u_c)} + \mu d_2 + \delta D(u_c)}{\chi\varphi(u_c)}, \tag{4.13}$$

such that no unstable modes exist if ν is below this critical number ν_c , whereas unstable modes are possible when ν is beyond this critical value ν_c [see Fig. 4(a) for the dispersion relation]. Furthermore, if we consider ν_c as a function of γ and recall the proof of Theorem 4.2, we can show that the critical value ν_c of the growth rate decreases as the parameter γ increases. This outcome is consistent with the biological context that, increasing the growth rate ν of the chemoattractant results in a higher concentration of chemoattractant, which makes the system more unstable.



(a)



(b)

FIG. 4. (a). Dispersion relation (4.5) as the parameter ν passes through the bifurcation value $\nu_c=10.18$, where $\gamma=4, d_1=0.1, d_2=1.0, u_c=2.0, \bar{u}=4.0, \mu=4.0, \delta=10.0, \chi=0.5$. (b) Dispersion relation (4.5) as the parameter δ passes through the bifurcation value $\delta_c=4.04$, where $\gamma=2, d_1=0.1, d_2=1.0, u_c=2.0, \bar{u}=4.0, \mu=10, \nu=20, \chi=0.5$.

Remember that the critical number ν_c is not necessarily a bifurcation value due to the discrete nature of the unstable modes. But we can formally obtain the desired bifurcation value for ν by performing the same analysis as for χ in Sec. IV A and obtain a bifurcation theorem similar with Theorem 4.1. To avoid repetition, we do not provide details here.

C. Bifurcation with decay rate δ

In the model (4.3), the parameter δ stands for the decay (degradation) rate of the chemoattractant, and the uniform steady state (u_s, v_s) depends on δ . If we perform the similar linear stability analysis as we did in previous sections, it is easy to derive a critical value for δ as

$$\delta_c = \frac{(\sqrt{\nu\chi\varphi(u_c)} - \sqrt{\mu d_2})^2}{d_1 D(u_c)}, \tag{4.14}$$

such that when $\delta > \delta_c$, there do not exist unstable modes, whereas unstable modes can be expected when $\delta < \delta_c$. Now, if we regard the death rate δ as a dynamical parameter, the dispersion relation of Eq. (4.5) as δ passes through the critical value δ_c , as shown in Fig. 4(b). Here the plot of the dispersion relation for δ in Fig. 4(b) has some difference in appearance compared to the plot of the dispersion relation for ν in Fig. 4(a). From Fig. 4(a), we see that all eigenvalues λ take the same value at $k^2=0$ for any dynamical parameter ν . However, Fig. 4(b) shows that the eigenvalue λ has a different value at $k^2=0$ for each different dynamical parameter δ . In fact, from Eq. (4.5), when $k^2=0$, we have

$$\lambda^2 + (\mu + \delta)\lambda + \mu + \delta = 0. \tag{4.15}$$

It is clear that Eq. (4.15) is independent of parameter ν but dependent on parameter δ .

Now we examine the relationship between the critical value δ_c and squeezing exponent γ . We still use the notation in Sec. IV A and rewrite Eq. (4.14) as follows:

$$\delta_c^{1/2} = \sqrt{\frac{1}{d_1(1 + \gamma\sigma^\gamma M(\gamma))}} (\sqrt{\nu\chi u_c} - \sqrt{\mu d_2 M(\gamma)}).$$

In Sec. IV A, we have shown that functions $M(\gamma)$ and $\gamma\sigma^\gamma M(\gamma)$ are decreasing with respect to γ . Then, it is easy to see that δ_c , as a function of γ , is increasing, which is in contrast to the critical growth rate ν_c that is a decreasing function of γ . This is in agreement with the biological interpretation. When increasing the squeezing exponent, the critical death rate becomes larger and hence pattern formation can allow for faster dilution of chemicals. As a consequence, pattern formation is easier to form.

V. NUMERICAL SIMULATION IN ONE DIMENSION

In this section, we will numerically investigate pattern formation for model (4.3). Unless stated otherwise, throughout this section, we assume zero-flux boundary conditions. For $\gamma=1$, numerical solutions have been shown by Painter and Hillen in Ref. 17. In the case of zero kinetics ($f(u, v) = 0$), Painter and Hillen found a typical behavior of merging of local peaks (also called coarsening process). In the paper by Potapov and Hillen,²² these local peaks were identified as metastable steady states and in the paper by Dolak *et al.*,^{32,34} a singular perturbation analysis around these transient patterns was given. These patterns are similar to coarsening patterns obtained for the Brusselator model,³³ where a nonlinear stability analysis was performed. If cell kinetics were included in the model, in addition to the merging of peak patterns, the emerging of new local maxima was observed also by Painter and Hillen.¹⁷ In this article, we particularly focus on the effect of nonlinear squeezing probability $q(u) = 1 - (u/\bar{u})^\gamma$ through $\gamma > 1$ on the merging and emerging process. We obtain a similar patterning process as the linear diffusion case ($\gamma=1$) in Ref. 17, and our results, confirm that merging and emerging processes are very typical patterning processes for the volume filling chemotaxis model.

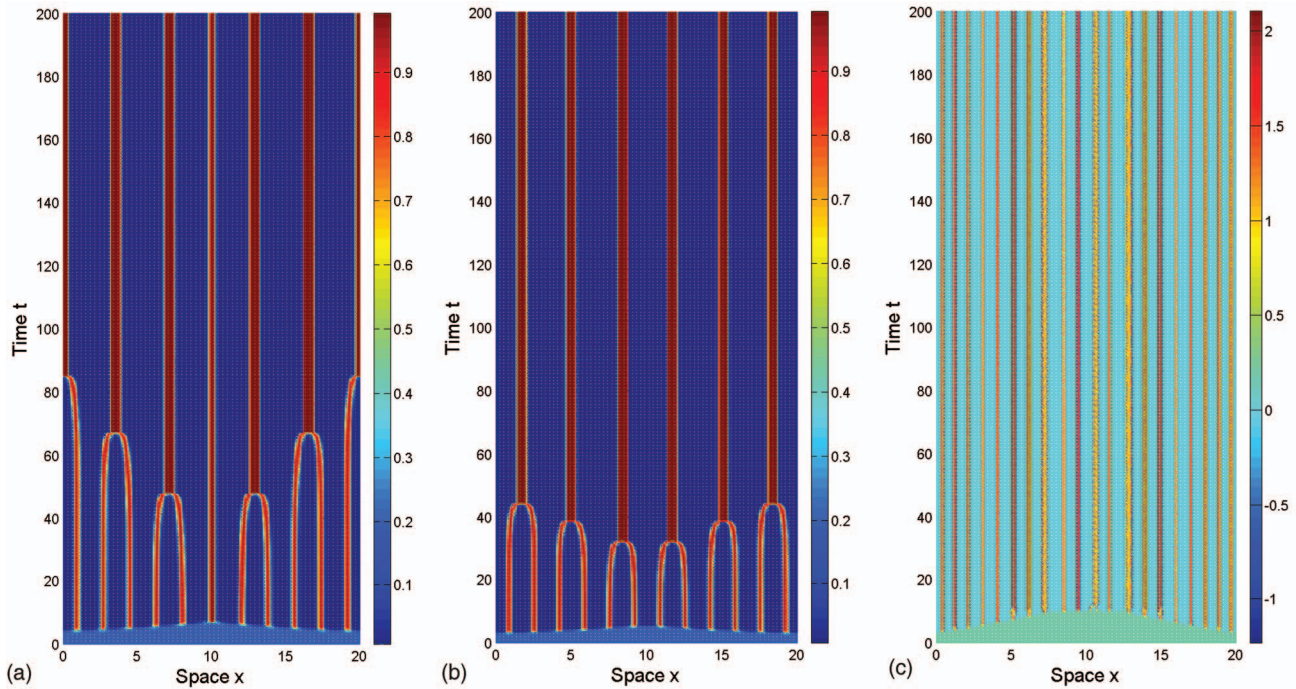


FIG. 5. (Color) Space-time evolution of cell density for model (4.3) with zero kinetics, with initial value that is set as the small perturbation of the homogeneous solution $u_0=0.2$ and with $\delta=10, \bar{u}=1.0, u_c=0.5, d_2=1.0$: (a) $\nu=40, d_1=0.25, \gamma=1, \chi=2$. (b) $\nu=40, d_1=0.25, \gamma=2, \chi=2$. (c) $\nu=30, d_1=0.01, \gamma=2, \chi=1$.

A. Zero cell kinetics

In this section, we will consider the nonlinear diffusion volume filling chemotaxis model (1.9) with cell kinetics $f(u, v)=0$ and $g(u, v)=\nu u - \delta v$ as well as nonlinear squeezing probability function $q(u)=1-(u/\bar{u})^\gamma, \gamma>1$. Then, the cell density is conserved due to no cell growth and death. Again, we look at the stability of the homogeneous steady state $(u_s, \nu u_s/\delta)$. Note that condition (3.4) is not satisfied in the case of $f=0$, however, the instability region can be explicitly determined by performing standard linear stability analysis as before,

$$\chi > \frac{\bar{u}^\gamma + (\gamma - 1)u_s^\gamma d_1 \delta}{u_s \bar{u}^\gamma (\bar{u}^\gamma - u_s^\gamma) \nu} \tag{5.1}$$

Under this condition, unstable wave modes can be expected. From Eq. (5.1), we see that the cell density is crucial for pattern formation. At high or low initial cell density u_s , the system tends to be stable to spatial perturbations.

Some typical numerical simulation examples are shown in Fig. 5. In Fig. 5(a), we choose squeezing exponent $\gamma=1$ and then the diffusion of the system (3.8) becomes linear. In Fig. 5(b), we choose $\gamma=2$ and the diffusion of the system (3.8) is then nonlinear. For both cases, we observe some initial merging process, which stops, and a new time-independent peak pattern appears. Actually, similar merging dynamics appears for other crowding exponents $\gamma>1$ (not shown).

In Fig. 5(c), we significantly reduce the cell diffusion parameter d_1 , which leads to a persistent steady state without observable merging dynamics.

B. Nonzero cell kinetics

From the above numerical analysis, we see that without cell kinetics we obtain multiple aggregations, which undergo a merging process. In this section, we include the effect of cell kinetics into the model and explore whether or not stable multipeak aggregation patterns can develop. We suppose that cells follow logistic growth $f(u, v)=\mu u(1-u/u_c)$. Production term $g(u, v)$ and squeezing probability $q(u)$ are chosen as before. Then the model is the same as Eq. (4.3).

The nontrivial uniform steady state of Eq. (4.3) is given by $(u_s, v_s)=(u_c, \nu u_c/\delta)$, and the instability region of this steady state is determined by condition (4.6). The graph of the dispersion relation now corresponds to Fig. 1(a). Thus, low wave modes might be stable to spatial perturbation, and higher wave modes may develop multipeak solutions, which is in contrast to the case of zero kinetics, where low wave modes might be unstable. We choose a set of parameters, such that the instability condition (4.6) is satisfied, and present the numerical simulation in Fig. 6. We first choose parameters deep in the instability region and it was shown that multiple peaks develop and that these peaks exist indefinitely [see Figs. 6(b) and 6(c)]. Numerical simulation shows that a time-independent persistent spatial pattern might not exist and patterns demonstrate an interesting pattern interaction process of merging and emerging, where neighboring aggregations join to form a single aggregation resulting in a large interval of low cell density. In the low density regions, new cell aggregations subsequently arise, which is in contrast to the zero kinetics case in which only a merging process was observed. When the parameters are chosen close to the stability/instability boundary, solutions can stabilize into

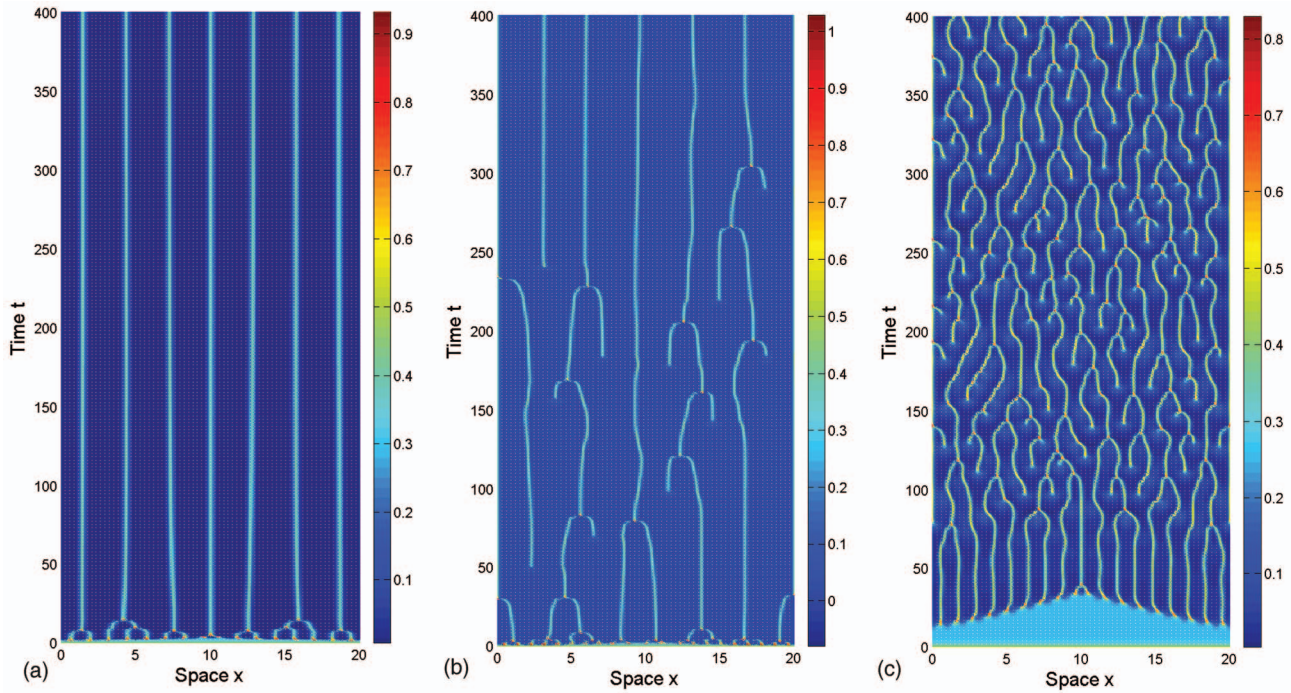


FIG. 6. (Color) Space-time evolution of cell density for model (4.3) for different choices of parameters. (a) $d_1=0.25, d_2=1, \nu=10, \delta=10, \bar{u}=1.0, u_c=0.25, \mu=0.5, \chi=10, \gamma=2$. Simulations indicate that a fixed spatial pattern exists as peaks persist and grow. Here are seven peaks. (b) $d_1=0.25, d_2=1, \nu=10, \delta=10, \bar{u}=1.0, u_c=0.25, \mu=0.5, \chi=20, \gamma=2$. (c) $d_1=0.01, d_2=1, \nu=10, \delta=10, \bar{u}=1.0, u_c=0.25, \mu=0.5, \chi=1, \gamma=2$. In (b) and (c), typical merging and emerging patterns develop. The parameters chosen in (a) are closer to the stability region than those chosen in (b) and (c). All simulations use the domain size as $[0, 20]$.

a time-independent spatial pattern [see Fig. 6(a), where a seven-peak pattern evolves]. However, there are no local peaks emerging during the evolution. In Fig. 6(c), we choose very small diffusive rate d_1 and get a more complex pattern due to high chemotactic effects.

The evolution of merging and emerging peak solutions is presented in Fig. 7. We see that peaks are capped by the crowding capacity \bar{u} due to the volume filling effects. For zero kinetics [see Fig. 7(a)], after some time, peaks merge into some stationary peaks. For the nonzero kinetics case [see Fig. 7(b)], we see that initially solution tends to blow up (very sharp) but the volume filling mechanism prevents blowup and then solutions stay bounded to form complex merging and emerging patterns.

VI. DISCUSSION

In this paper, we include a nonlinear squeezing probability function $q(u)$, which reflects elastic properties of cells, into a volume filling chemotaxis model and prove the global existence of classical solutions to the resulting model. We show that the cell density will stay below the crowding capacity \bar{u} if the initial cell density is less than this crowding capacity. We carry out conditions of pattern formation for the general volume filling chemotaxis model. Moreover, we apply a particular choice Eq. (4.1) of $q(u)$ into the model to perform the linear stability analysis and study the underlying bifurcation for different parameters. One-dimensional numerical simulations are presented for both zero cell kinetics and nonzero cell kinetics. Merging and emerging dynamics are observed under different parameter values. We find that the squeezing exponent γ has no huge effect on the spa-

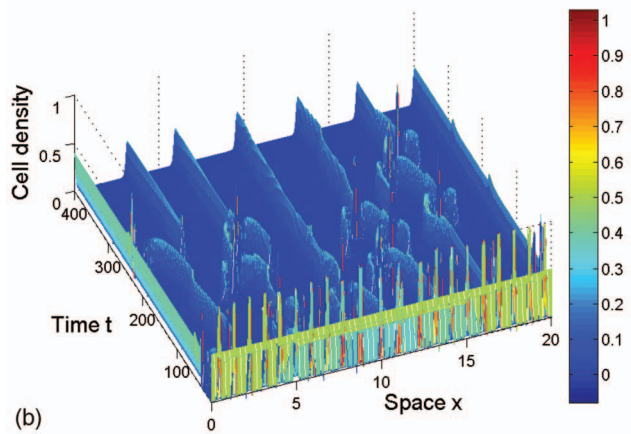
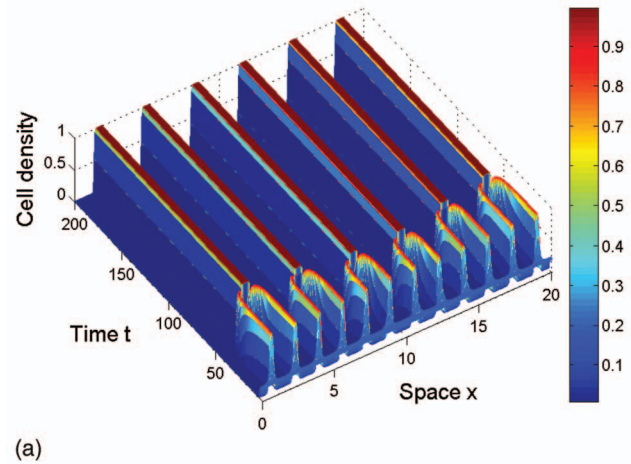


FIG. 7. (Color) Evolution of merging and emerging local peaks. (a) Zero cell kinetics, where $\nu=40, \delta=10, \bar{u}=1.0, u_c=0.5, d_1=0.25, d_2=1.0, \gamma=1, \chi=2$. (b) Nonzero cell kinetics, where $d_1=0.25, d_2=1, \nu=10, \delta=10, \bar{u}=1.0, u_c=0.25, \mu=0.5, \chi=20, \gamma=2$.

tiotemporal dynamics. The merging and emerging process can be observed for all values of $\gamma \geq 1$; the limit state, however, depends on γ .

The parameter γ has been included to describe elastic properties of cells. The case of $\gamma=1$ corresponds to solid blocks (see the car-parking problem in Ref. 21), whereas $\gamma \rightarrow \infty$ corresponds to cells being fluids, which can fill all open space. The critical chemosensitivity χ_c is decreasing in γ ; hence, increasing γ is destabilizing the system. If γ is large, chemotaxis has a large effect and more cells can still enter into a crowded region and make chemotactic aggregation more pronounced.

Comparing Figs. 7(a) and 7(b), we can conclude that the emerging process is due to cell growth. It is of interest to further study the merging and emerging process in more details. The merging and emerging patterns in Fig. 6(b) seem to have a dominating wavelength so that neither too many nor too few local maxima arise. In Ref. 22 some scaling and numerical analyses were applied to describe the transition region and the local peaks were identified with metastable steady states. For the merging process (no kinetics), a qualitative analysis was given by Dolak and Schmeiser³² using a singular perturbation argument. It would be interesting to apply their methods to study the merging-emerging process as observed above. A detailed analysis will be given in a forthcoming paper.

ACKNOWLEDGMENT

We are grateful to K. Painter for fruitful discussions about cell crowding, cell elasticity, and the car-parking problem. We thank D. Wrzosek for helpful remarks about *fast diffusion* problems. Thanks are also extended to T. Kolokolnikov, who brought our attention to similar merging patterns for the Brusselator model. The work of Z.W. is supported by the F. S. Chia scholarship of the University of Alberta and China Government Award for Outstanding Self-financed Students Abroad. The research of T.H. is supported by NSERC.

¹R. Tyson, S. R. Lubin, and J. Murray, "A minimum mechanism for bacterial pattern formation," *Proc. R. Soc. London, Ser. B* **266**, 299–304 (1999).

²R. Tyson, S. R. Lubin, and J. Murray, "Models and analysis of chemotactic bacterial patterns in a liquid medium," *J. Math. Biol.* **38**, 359–375 (1999).

³D. Woodward, R. Tyson, M. Myerscough, J. Murray, E. Budrene, and H. Berg, "Spatiotemporal patterns generated by *Salmonella typhimurium*," *Biophys. J.* **68**, 2181–2189 (1995).

⁴P. Friedl, S. Borgmann, and E. Bröcker, "Amoeboid leucocyte crawling through extracellular matrix: Lessons from the *Dictyostelium* paradigm of cell movement," *J. Leukoc. Biol.* **70**, 491–509 (2001).

⁵K. Painter, H. G. Othmer, and P. K. Maini, "Stripe formation in juvenile *Pomacanthus* via chemotactic response to a reaction-diffusion mechanism," *Proc. Natl. Acad. Sci. U.S.A.* **96**, 5549–5554 (1999).

⁶H. Byrne and M. Chaplain, "Mathematical models for tumour angiogenesis-numerical simulations and nonlinear-wave equations," *Bull. Math. Biol.* **57**, 461–485 (1995).

⁷E. Keller and L. Segel, "Model for chemotaxis," *J. Theor. Biol.* **30**, 225–234 (1971).

⁸D. Horstmann, "From 1970 until present: The Keller-Segel model in

chemotaxis and its consequences. I," *Jahresberichte der Deutschen Mathematiker Vereinigung* **105**, 103–165 (2003).

⁹D. Horstmann, "From 1970 until present: The Keller-Segel model in chemotaxis and its consequences. II," *Jahresberichte der Deutschen Mathematiker Vereinigung* **106**, 51–69 (2004).

¹⁰M. Mimura and T. Tsujikawa, "Aggregating pattern dynamics in a chemotaxis model including growth," *Physica D* **230**, 499–543 (1996).

¹¹K. Osaki, T. Tsujikawa, A. Yagi, and M. Mimura, "Exponential attractor for a chemotaxis-growth system of equations," *Nonlinear Analysis*. **51**, 119–144 (2002).

¹²P. Biler, "Local and global solvability of some parabolic systems modeling chemotaxis," *Adv. Math. Sci. Appl.* **8**, 715–743 (1998).

¹³K. C. Chen, R. M. Ford, and P. T. Cummings, "Mathematical models for motile bacterial transport in cylindrical tubes," *J. Theor. Biol.* **195**, 481–504 (1998).

¹⁴H. G. Othmer and A. Stevens, "Aggregation, blowup and collapse: The ABC's of taxis in reinforced random walks," *SIAM J. Appl. Math.* **57**, 1044–1081 (1997).

¹⁵T. Hillen, K. Painter, and C. Schmeiser, "Global existence for chemotaxis with finite sampling radius," *Discrete Contin. Dyn. Syst., Ser. B* **7**, 125–144 (2007).

¹⁶M. Luca, A. Chaves-Ross, L. Edelstein-Keshet, and A. Mogilner, "Chemotactic signaling, microglia, and Alzheimer's disease senile plaques: Is there a connection?" *Bull. Math. Biol.* **65**, 693–730 (2003).

¹⁷K. Painter and T. Hillen, "Volume-filling and quorum-sensing in models for chemosensitive movement," *Canadian Applied Mathematics Quarterly*. **10**, 501–543 (2002).

¹⁸K. Painter, P. K. Maini, and H. G. Othmer, "Complex spatial patterns in a hybrid chemotaxis reaction-diffusion model," *J. Math. Biol.* **41**, 285–314 (2000).

¹⁹T. Hillen, J. Renclawowicz, and Z. Wang, "Analysis of an attraction-repulsion chemotaxis model" (unpublished).

²⁰T. Hillen and K. Painter, "A comparison of chemotaxis models" (unpublished).

²¹R. Schaaf and J. Talbot, "Surface exclusion effects in adsorption processes," *J. Chem. Phys.* **91**, 4401–4409 (1989).

²²A. Potapov and T. Hillen, "Metastability in chemotaxis models," *J. Dyn. Differ. Equ.* **17**, 293–330 (2005).

²³Z. Wang, "Mathematical models for cell movements," Ph.D. thesis, University of Alberta, 2007.

²⁴T. Hillen and K. Painter, "Global existence for a parabolic chemotaxis model with prevention of overcrowding," *Adv. Appl. Math.* **26**, 280–301 (2001).

²⁵D. Wrzosek, "Global attractor for a chemotaxis model with prevention of overcrowding," *Nonlinear Analysis*. **59**, 1293–1310 (2004).

²⁶H. Amann, "Dynamic theory of quasilinear parabolic equations II: Reaction-diffusion systems," *Diff. Integral Eq.* **3**, 13–75 (1990).

²⁷H. Amann, "Dynamic theory of quasilinear parabolic equations III: Global existence," *Math. Z.* **202**, 219–250 (1989).

²⁸H. Amann, "Nonhomogeneous linear and quasilinear elliptic and parabolic boundary value problems," in *Function Spaces, Differential Operators and Nonlinear Analysis*, edited by H. J. Schmeisser, H. Triebel (Teubner, Stuttgart, 1993), pp. 9–126.

²⁹D. Horstmann, "Lyapunov functions and L^p estimates for a class of reaction-diffusion systems," *Colloq. Math.* **87**, 113–127 (2001).

³⁰G. M. Lieberman, *Second Order Parabolic Differential Equations* (World Scientific, Singapore, 1996).

³¹J. D. Murray, *Mathematical Biology* (Springer-Verlag, Berlin, 1993).

³²Y. Dolak and C. Schmeiser, "The Keller-Segel model with logistic sensitivity function and small diffusivity," *SIAM J. Appl. Math.* **66**, 286–308 (2005).

³³T. Kolokolnikov, T. Erneux, and J. Wei, "Mesa-type patterns in the one-dimensional Brusselator and their stability," *Physica D* **214**, 63–77 (2006).

³⁴M. Burger, M. Francesco, and Y. Dolak, "The Keller-Segel model for chemotaxis with prevention of overcrowding: Linear and nonlinear diffusion," *SIAM J. Math. Anal.* **38**, 1288–1315 (2006).

³⁵D. Wrzosek, "Long time behavior of solutions to a chemotaxis model with volume filling effects," *Proc. - R. Soc. Edinburgh, Sect. A: Math.* **136**, 431–444 (2006).